JACS
JOURNAL OF THE AMERICAN CHEMICAL SOCIETY
Article
pubs.acs.org/JACS

A Highly Compliant Protein Native State with a Spontaneous-like Mechanical Unfolding Pathway

Pétur O. Heidarsson,[†] Immanuel Valpapuram,[‡] Carlo Camilloni,[§] Alberto Imparato,[∥] Guido Tiana,[#] Flemming M. Poulsen,[†] Birthe B. Kragelund,[†] and Ciro Cecconi*[,⊥]

[†]Structural Biology and NMR Laboratory, Department of Biology, University of Copenhagen, Ole Maaløes Vej 5, 2200 Copenhagen N, Denmark

[‡]Department of Physics, University of Modena and Reggio Emilia, Via Guiseppe Campi, 41125 Modena, Italy

[§]Department of Chemistry, University of Cambridge, Lensfield Road, Cambridge CB2 1EW, United Kingdom

[∥]Department of Physics and Astronomy, University of Aarhus, Ny Munkegade, Building 1520, 8000 Aarhus C, Denmark

[#]Department of Physics, University of Milano and INFN, Via Celoria 13, 20133 Milano, Italy

[⊥]CNR-Nano, Department of Physics, University of Modena and Reggio Emilia, Via Guiseppe Campi, 41125 Modena, Italy

Supporting Information

ABSTRACT: The mechanical properties of proteins and their force-induced structural changes play key roles in many biological processes. Previous studies have shown that natively folded proteins are brittle under tension, unfolding after small mechanical deformations, while partially folded intermediate states, such as molten globules, are compliant and can deform elastically a great amount before crossing the transition state barrier. Moreover, under tension proteins appear to unfold through a different sequence of events than during spontaneous unfolding. Here, we describe the response to force of the four-α-helix acyl-CoA binding protein (ACBP) in the low-force regime using optical tweezers and ratcheted molecular dynamics simulations. The results of our studies reveal an unprecedented mechanical behavior of a natively folded protein. ACBP displays an atypical compliance along two nearly orthogonal pulling axes, with transition states located almost halfway between the unfolded and folded states. Surprisingly, the deformability of ACBP is greater than that observed for the highly pliant molten globule intermediate states. Furthermore, when manipulated from the N- and C-termini, ACBP unfolds by populating a transition state that resembles that observed during chemical denaturation, both for structure and position along the reaction coordinate. Our data provide the first experimental evidence of a spontaneous-like mechanical unfolding pathway of a protein. The mechanical behavior of ACBP is discussed in terms of topology and helix propensity.

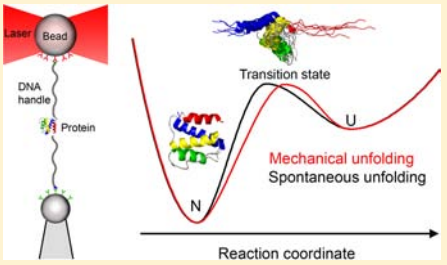

INTRODUCTION

The reaction of proteins to mechanical force with loss or gain of structures under tension plays an important role in diverse biological processes.[1] Different proteins respond to force differently. Some proteins resist mechanical stress to prevent cells moving apart from one another (e.g., cadherin) or to preserve the integrity of cells and tissues (e.g., α-actinin and tenascin).[2,3] Other proteins exploit mechanical strain to translocate from one cellular compartment to another or to enter into proteasomes for degradation.[4] Mechanosensors respond to mechanical stimuli undergoing conformational changes that initiate intracellular signaling cascades or open membrane channels.[5] Understanding the basic principles that govern the behavior of a protein under tension is important for delineation of the mechanisms by which fundamental biological processes are influenced and regulated by force.

Advances in single molecule force spectroscopy techniques, such as optical tweezers and atomic force microscopy (AFM), have recently made it possible to study the response of proteins to force in great detail.[6] Using these methods, it is possible to apply tiny forces directly onto individual molecules and describe their unfolding/refolding trajectories along a reaction coordinate defined by the points of force application.[7−10] These studies have provided a wealth of new information about the mechanical properties of natively and partially folded protein states. We now know for example the magnitude of the forces that hold together the three-dimensional structures of different proteins and the compliance of their native states (N), that is, how much they can be deformed along the pulling axis without crossing the transition state (TS) barrier.[7,8,11−15] The larger the distance ($x^{\ddagger}_{u}$) separating N and TS is, the more pliant a protein structure is. Natively folded single-domain proteins appear to be brittle, as they unfold after small deformations ($x^{\ddagger}_{u}$ < 2 nm).[7,8,11,12] It follows, therefore, that along the reaction coordinate their TSs are located much closer to N than to the unfolded state (U), and the ratio between $x^{\ddagger}_{u}$ and the N to U distance, previously defined as "mechanical" Tanford β-value

Received: June 16, 2012
Published: September 24, 2012

   dx.doi.org/10.1021/ja305862m | J. Am. Chem. Soc. 2012, 134, 17068−17075

(herein referred to as $m\beta_{Tu}$),[16,17] is small ($m\beta_{Tu} \sim 0.05-0.1$).[11] On the other hand, molten globules appear to be mechanically compliant. These intermediate states, which characterize the folding trajectories of many proteins, are very pliant under tension and they can be stretched for several nanometers before crossing the TS barrier, resulting in higher $m\beta_{Tu}$ values of ~0.3.[16] It has been speculated that this large deformability is a consequence of their unique molecular structures that are stabilized mainly by short-range interactions and weak nonstereospecific tertiary contacts.[7,16]

Force spectroscopy, in combination with molecular dynamics (MD) simulations, has also provided information about the sequence of events characterizing the mechanical denaturation of a molecule.[18,19] These studies have shown that in the high-force regime explored in AFM experiments proteins under tension unfold through pathways that significantly differ from those probed during chemical/thermal denaturation (spontaneous unfolding), and populate different transition states.[20−22] These studies, however, have also suggested that under milder mechanical perturbations, forced and spontaneous unfolding could resemble each other.[23] Classical MD simulations of mechanical unfolding have been hampered by the fact that at small forces of only a few piconewton (pN) proteins unfold on time scales that are not reachable by standard computational techniques. In fact, a theoretical description of mechanical unfolding has so far been carried out only with very simple models,[24−26] with coarse-grained interactions, or using forces that are orders of magnitude larger than those used in force spectroscopy experiments.[27,28] This problem can be partially solved with ratcheted MD simulations,[29] which are able to extract the sequence of conformational changes between given points of the conformational space at low forces, provided that a good reaction coordinate is chosen (Supporting Information). The caveat is that there is no linear correspondence between the simulation time and real time of the trajectories, and it is not possible to determine the free energy change of the system. Still, ratcheted MD simulations can be used to elucidate the structure and position of the TS along the unfolding reaction coordinate at atomic resolution. This technique has proven successful in studying the sequence of events during protein unfolding[30,31] and during the spontaneous folding of protein G, chymotrypsin inhibitor 2 and acyl-CoA binding protein (ACBP).[32]

In the present work, we characterize the behavior of individual ACBP molecules in the low-force regime using optical tweezers and ratcheted MD simulations. ACBP is a topologically simple and highly conserved 86 amino acid residue protein made of four α-helices organized in a unique up-down-down-up skewed bundle (Figure 1A).[33] Under our experimental conditions, ACBP unfolds in a two-state manner and displays an unusual mechanical compliance along two nearly orthogonal axes. Interestingly, the $m\beta_{Tu}$-values measured for ACBP along both axes are larger than those reported for the highly pliant molten globule states. When manipulated from the N- and C-termini in optical tweezers experiments and in MD simulations, ACBP unfolds by populating a TS located more than 5 nm from N. The structure and position of the TS along the reaction coordinate resemble those of the TS observed in bulk studies. Our results provide the first experimental evidence that in the low-force regime a protein can denature through a sequence of events that resembles that observed during spontaneous unfolding induced by chemical or thermal denaturants.

MATERIALS AND METHODS

Protein Expression, Purification, and Sample Preparation. The double cysteine variants $ACBP^{1-86}$ and $ACBP^{46-86}$ were expressed in *Escherichia coli* BL21(DE3)-pLysS cells transformed with a pET3a expression vector containing the mutated bovine ACBP gene.[34] Purification was performed as previously described.[35] Attachment of DNA to proteins and coupling of protein−DNA chimeras to beads were performed exactly as described.[36]

Optical Tweezers Experiments. All experiments were performed using a custom-built optical tweezers instrument with a dual-beam laser trap. The experiments were conducted at ambient temperatures in 10 mM Tris, 250 mM NaCl, 10 mM $CaCl_2$, 0.04% NaN_3, pH 7.0. A 3.10 μm antidigoxigenin-coated bead (Spherotec) was held in the optical trap, while a 2.18 μm streptavidin-coated bead (Spherotec) was held at the end of a micropipet by suction. The force applied on the molecule was varied by moving the micropipet toward or away from the optical trap by means of a piezoelectric flexure stage (MAX311/M, Thorlabs, Newton, NJ). The force applied on the protein was determined by measuring the change in momentum flux of the light beams leaving the trap, while the extension of the molecule was determined by measuring the bead separation distance.[37] During force-ramp experiments,[38,39] the molecules are stretched and relaxed at constant speed (nm s^{-1}). Under our experimental conditions, above ~3 pN, the exerted force changes approximately linearly with time and thus the loading rate (pN s^{-1}) is approximately constant.[7,40,41] The applied force and molecule extension were recorded at a rate of 40 Hz. The single molecule nature of each experiment was confirmed by identifying the characteristic DNA overstretching transition at 67 pN.[7] In force-jump experiments, the force applied on the molecule was jumped between two set-point values and kept constant through a force-feedback mechanism. The dead-time (time of jump) was measured to be 60 ms. The average force was measured and compared with the desired force every 1 ms. Any difference between these forces was compensated by moving the micropipet with the piezoelectric flexure stage. In force-jump experiments, the applied force and molecule extension were recorded at a rate of 100 Hz.

Changes in Contour Length. Theoretical changes in contour lengths (ΔL_c) upon unfolding/refolding of ACBP were calculated as described.[7] Distances between the attachment points in the native structure were measured using the solution structure of ACBP (Protein Data Bank code 1NTI). Upon an unfolding or refolding event, ΔL_c was calculated as: (number of residues between the attachment points × 0.36 nm) − (distance between the attachment points in the native structure). We calculated a ΔL_c of 28.2 nm for $ACBP^{1-86}$, and 10.6 nm for $ACBP^{46-86}$. Fitting the worm-like chain (WLC) model to the force vs extension traces[7,41] yielded a ΔL_c of 26.8 ± 1.7 nm for $ACBP^{1-86}$ and a ΔL_c of 9.9 ± 0.8 for $ACBP^{46-86}$ (Figure S1).

Position of TS and Rate Constants from Force Spectroscopy Experiments. The two-state unfolding and refolding processes of ACBP were analyzed with the phenomenological Bell model, which postulates that the unfolding (k_u) and refolding (k_f) rate constants depend exponentially on force:[41,42]

$$k_u(F) = k_m k_u^0 \exp\left(\frac{F x_u^{\ddagger}}{k_B T}\right) \quad (1)$$

$$k_f(F) = k_m k_f^0 \exp\left(-\frac{F x_f^{\ddagger}}{k_B T}\right) \quad (2)$$

where k_u^0 and k_f^0 are the unfolding and refolding rate constants of the molecule at zero force, k_m is a "machine" constant that reflects the effect of instrumental factors, such as beads and molecular handles, on the measured rates,[41,43,44] F is the applied force, x_u and x_f are the distances from the TS to the folded and unfolded states, respectively, k_B is the Boltzmann constant and T is the absolute temperature. Force-jump data can be fitted using the logarithmic forms of eqs 1 and 2 to estimate rate constants and distances to the TS from the intercepts and slopes of the graphs, respectively (Figures 2E and 3C).[40] More

dx.doi.org/10.1021/ja305862m | J. Am. Chem. Soc. 2012, 134, 17068−17075

detailed expressions for the unfolding/refolding rates have been proposed,[45−48] that take into account the explicit dependence of the TS position on the applied force, and that extend eqs 1 and 2. Here, however, we stick to the Bell's formalism, as we wish to explore small force regimes, while deviation from eqs 1 and 2 can only be detected when one considers forces ranging over several orders of magnitude.

For a two-state system, in the case of force increasing linearly with time, an approach similar to that used to obtain eqs 1 and 2 gives the position of the TS and rate constants according to the following equations:[41,49]

$$\ln[r \ln[1/N(F, r)]] = \ln(k_m k_u^0 k_B T/x_u^{\ddagger}) + (x_u^{\ddagger}/k_B T)F \quad (3)$$

$$\ln[-r \ln[1/U(F, r)]] = \ln(k_m k_f^0 k_B T/x_f^{\ddagger}) - (x_f^{\ddagger}/k_B T)F \quad (4)$$

where $N(F,r)$ and $U(F,r)$ are the fraction of folded and unfolded molecules at the force F and loading rate r (pN s^{-1}). $N(F,r)$ and $U(F,r)$ can be calculated by integrating the unfolding and refolding force distributions over the corresponding range of forces. Equations 3 and 4 can be used to fit $\ln[r \ln[1/N(F,r)]]$ vs F, and $\ln[-r \ln[1/U(F,r)]]$ vs F to estimate distances to the TS and rate constants from the slope and intercept of the graphs, respectively (Figures 2C and 3B).

Since rate constants estimated through force spectroscopy experiments contain contributions from experimental parameters (k_m), they are difficult to interpret and cannot be compared directly to intrinsic rate constants of the protein. For this reason, rate constants were not included in Table 1.

Molecular Dynamics Simulations. Simulations were carried out starting from the NMR structure of ACBP[33] using the Amber03 force field[50] in its porting to Gromacs.[51] They were performed with a version of Gromacs 4.0.7[52] modified as described.[53] The protein was inserted in a parallel epipedal box of sides 4.8 × 4.8 × 20 nm and filled by 14 920 water molecules described by the TIP3p model. The temperature was kept to 300K by a Nosè-Hoover thermostat. Ratcheted MD simulations use the standard force field, to which a soft biasing potential (U_{rat}) is added which depends on the value y of the reaction coordinate in the harmonic form

$$U_{rat}(t) = \frac{1}{2}k(\rho(t) - \min_{t'<t}\rho(t'))^2 \quad (5)$$

where k is the harmonic constant, $\rho(t) = (y(t) - y_{target})^2$, y is the reaction coordinate (which is the distance between Cys1 and Cys86), and y_{target} is the desired/wanted ending point of the simulation (which is 20 nm for the unfolding simulations). If the value of k is small enough, the sequence of events obtained with ratcheted molecular dynamics is a good approximation of the actual trajectories. For each intensity value of the (constant) applied force, we generated different sets of six unfolding trajectories and analyzed the associated sequence of events and the structure of the TS (see Supporting Information for details).

RESULTS

Single Molecule Force Spectroscopy. Single ACBP molecules were manipulated by means of polystyrene beads (Figure 1). DNA molecular handles were attached to cysteine residues engineered either at the extreme termini (ACBP$^{1-86}$ variant) or at positions 46 and 86 (ACBP$^{46-86}$ variant), effectively pulling the protein along two roughly orthogonal axes (Figure 1A). The kinetics of the unfolding and refolding of both variants were studied through force-ramp and force-jump experiments.[40] During force-ramp experiments, the micropipet was moved at constant speeds (nm s^{-1}) to generate almost constant loading/relaxation rates of pulling (pN s^{-1}). When mechanically manipulated in force-ramp experiments, ACBP$^{1-86}$ unfolds at ∼10 pN and refolds at ∼3 pN (Figure 2A). The changes in contour length associated with these transitions are consistent with complete unfolding and refolding of the protein, indicating a two-state folding behavior of ACBP$^{1-86}$ (Figure S1, Materials and Methods). The transient intermediate states observed in bulk during the spontaneous folding of ACBP[54,55] are too short-lived ($\tau_f \sim 0.1$ ms and $\tau_u \sim 1$ ms) to be detected in our measurements. ACBP$^{1-86}$ was stretched and relaxed multiple times to generate unfolding and refolding force distributions (Figure 2B).

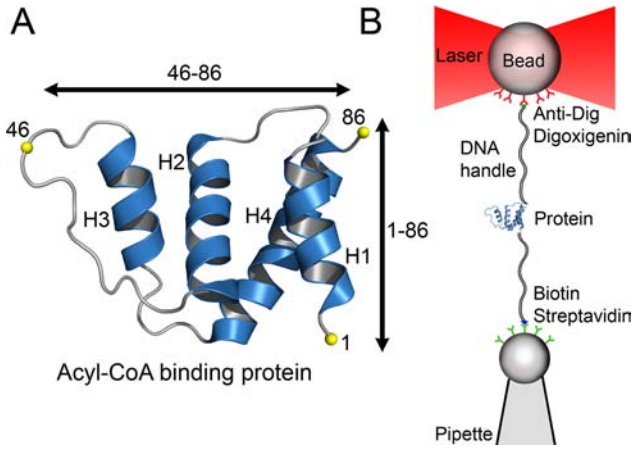

Figure 1. Structure of ACBP and experimental setup. (A) NMR structure of ACBP (Protein Data Bank code 1NTI). ACBP has a simple four-α-helical topology, with the helices arranged in a skewed up-down-down-up structure. The cysteine pairs 1−86 and 46−86 define two roughly orthogonal pulling axes, indicated by arrowhead lines. (B) Single ACBP molecules are manipulated by use of DNA handles attached to polystyrene beads. The protein is stretched and relaxed by moving the pipet relative to the optical trap.

The analysis of these data (Figure 2C) provided information on rate constants and position of the TS along the reaction coordinate (Materials and Methods).[41,49] The distances from TS to N ($x^{\ddagger}_u$) and from TS to U ($x^{\ddagger}_f$) were estimated to be 5.2 ± 0.2 and 6.7 ± 0.1 nm, respectively (Table 1). Similar information was obtained more directly through force-jump experiments. In these measurements the force is increased (jumped) or decreased (dropped) quickly to a preset value and kept constant with a feedback mechanism until an unfolding or refolding event is observed (Figure S3).[40] Rate constants can be measured at different forces directly from the distributions of the measured dwell-times (Figure 2D).[41] The force dependence of the rate constants can then be analyzed with Bell's model to extract information on kinetics (Figure 2E, Table 1 and Materials and Methods).[42,49] This analysis yielded an $x^{\ddagger}_u$ of 5.5 ± 0.6 nm, and $x^{\ddagger}_f$ of 6.5 ± 0.3 nm. The positions of the TS obtained with the two experimental methods are in good agreement within the statistical errors. Our data give an average $x^{\ddagger}_u$ for ACBP$^{1-86}$ of 5.35 ± 0.62 nm and an average mβ_{Tu} of 0.45 ± 0.06. These values are remarkably high, being significantly larger (3−15 times) than those found for previously studied natively folded proteins.[7,8,11,12] More interestingly, they are larger than the mβ_{Tu} reported for molten globules, that are considered to be extremely deformable intermediate states due to the lack of stereospecific tertiary contacts in their three-dimensional structures.[7,16]

To study the mechanical properties of ACBP along a different pulling axis, similar experiments were carried out with ACBP$^{46-86}$. This variant unfolded at ∼18 pN and refolded at ∼12 pN, through all-or-none transitions associated with changes in contour length consistent with complete unfolding and refolding of the molecular region subject to force (Figure

dx.doi.org/10.1021/ja305862m | J. Am. Chem. Soc. 2012, 134, 17068−17075

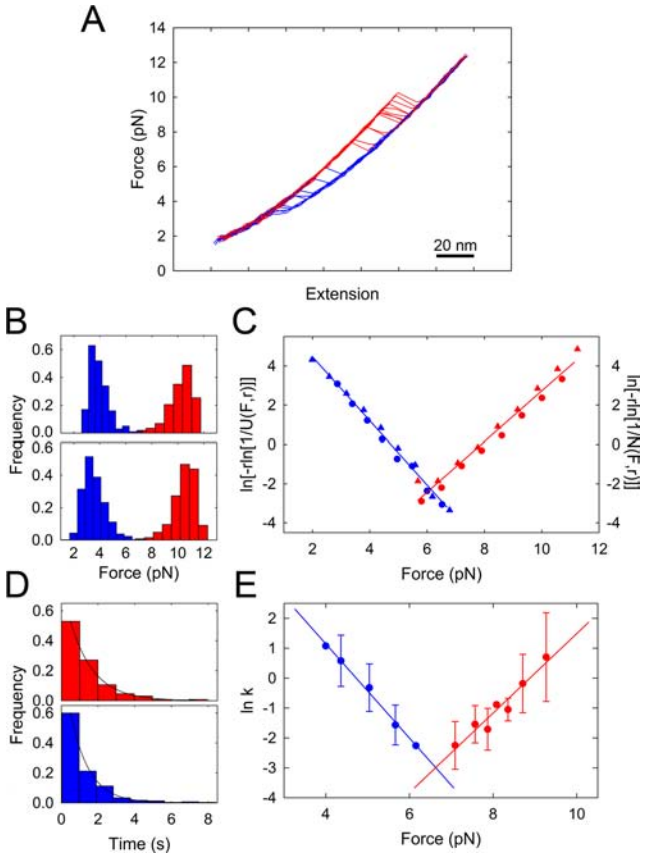

Figure 2. Force-ramp and force-jump experiments for ACBP$^{1-86}$. (A) Force vs extension cycles for ACBP$^{1-86}$. The molecule was stretched (red) and relaxed (blue) multiple times at a loading rate (r) of 15 pN s^{-1}. Unfolding and refolding events generate sudden changes in the extension of the molecule that give rise to discontinuities (rips) in the recorded traces. (B) Distributions of unfolding (red) and refolding (blue) forces. Upper panel: Unfolding, r = 15 pN s^{-1}, N = 295, refolding, r = 8.5 pN s^{-1}, N = 293. Lower panel: Unfolding, r = 45 pN s^{-1}, N = 601, refolding, r = 15 pN s^{-1}, N = 150. (C) Plots of ln[r ln[1/N]] and ln[$-r$ ln[1/U]] vs force, where N and U are the folded and unfolded fractions, respectively. Solid circles represent unfolding (red) and refolding (blue) data collected at 15 and 8.5 pN s^{-1}, respectively. Triangles represent unfolding (red) and refolding (blue) data collected at 45 and 15 pN s^{-1}, respectively. Data acquired at different loading rates appear to overlap. Best fit values for $x^{\ddagger}_u$ and $x^{\ddagger}_f$ are reported in Table 1. Similar $x^{\ddagger}_u$ and $x^{\ddagger}_f$ values were obtained by fitting unfolding and refolding distributions directly to probability distribution functions (Figure S2).[49] (D) Dwell-time histograms of the folded (red, N = 387) and unfolded (blue, N = 302) states measured at 8.6 and 5 pN respectively. Single exponential fits to the data (solid lines) demonstrate the first-order nature of the unfolding/refolding transitions and yielded a $k_m k_u$ of 0.79 ± 0.03 s^{-1}, and $k_m k_f$ of 0.99 ± 0.03 s^{-1} (Materials and Methods). (E) Natural logarithm of the unfolding (red) and refolding (blue) rate constants measured through force-jump experiments at different forces. Solid lines are fits with Bells model (Table 1 and Materials and Methods).

3A and Materials and Methods). As for ACBP$^{1-86}$, force and lifetime distributions of ACBP$^{46-86}$ were analyzed to extract

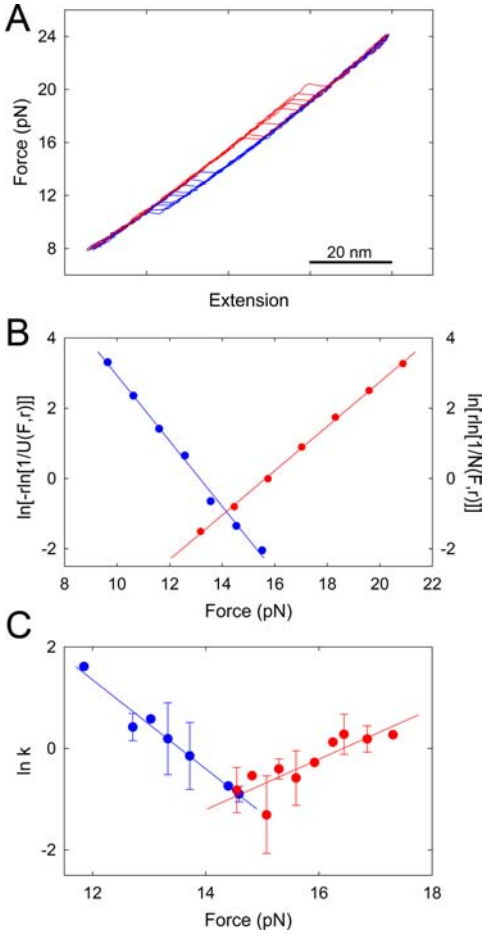

Figure 3. Force-ramp and force-jump experiments for ACBP$^{46-86}$. (A) Force vs extension cycles for ACBP$^{46-86}$ at 13 pN s^{-1}. The size of the transitions is consistent with complete unfolding and refolding of the protein region subject to force. (B) Plots of ln[r ln[1/N]] and ln[$-r$ ln[1/U]] vs force. Best fit values for $x^{\ddagger}_u$ and $x^{\ddagger}_f$ are reported in Table 1. Similar $x^{\ddagger}_u$ and $x^{\ddagger}_f$ values were obtained by fitting unfolding and refolding distributions to probability distribution functions (Figure S4).[49] (C) Natural logarithm of the unfolding (red) and refolding (blue) rate constants vs force. Solid lines are fits with Bells model (Table 1 and Materials and Methods).

information on the kinetics of the unfolding and refolding processes (Figure 3B,C, Figure S4, and Table 1). Given the number of residues between the points of force application, the value of $x^{\ddagger}_u$ for ACBP$^{46-86}$ is remarkably large (2.4 ± 0.7 nm), and the mβ_{Tu} value is similar to that measured for ACBP$^{1-86}$ (0.39 ± 0.13). These data show that the unusual compliance of ACBP is an intrinsic property of its three-dimensional structure and not a property of the pulling axis.

Table 1. TS Positions and Mechanical Tanford β-Values for ACBP

variant	experiment	$x^{\ddagger}_u$ (nm)	$x^{\ddagger}_f$ (nm)	<mβ_{Tu}>	<mβ_{Tf}>
ACBP$^{1-86}$	Force-ramp	5.2 ± 0.2	6.7 ± 0.1	0.45 ± 0.06	0.55 ± 0.06
	Force-jump	5.5 ± 0.6	6.5 ± 0.3		
ACBP$^{46-86}$	Force-ramp	2.6 ± 0.1	3.8 ± 0.1	0.39 ± 0.13	0.61 ± 0.05
	Force-jump	2.1 ± 0.4	3.6 ± 0.3		

dx.doi.org/10.1021/ja305862m | J. Am. Chem. Soc. 2012, 134, 17068−17075

Ratcheted Molecular Dynamics. State-of-the-art ratcheted MD simulations of the mechanical denaturation of ACBP$^{1-86}$ in explicit solvent were carried out at constant forces of 12, 30, and 60 pN (Materials and Methods and Supporting Information). For each value of the force, six unfolding trajectories were simulated. The sequence of forced denaturation events at 12 pN is visualized in Figure 4A. Unfolding starts with disruption of tertiary contacts between H1 and the rest of the protein, and subsequently intrahelical contacts in H1 are lost. Then H4 starts losing both its intrahelical and tertiary contacts. The structure involving H2 and H3, which is not subject directly to force, is the last to yield before complete unfolding. However, in our simulations, unfolding of H2 and H3 proceeds in a heterogeneous way, with no specific unfolding sequence, as it is evident at d = 16 nm. A more detailed analysis of the unfolding process can be obtained by the order of native-contact disruption at a residue level (Figure S5 and Supporting Information). The very first native contacts to be lost are located at both ends of H1 and between contacts K8−D78 (H1−H4), P19−L27 (L1−H2), F5−L30 (H1−H2) and T17−Y84 (L1−H4).

Some small rearrangements take place also in H2 (S20−E23, L24−L27), while H3 remains intact. Among the last native contacts to be disrupted are Q33−A69, Q33−L61 and V36−W58.

From ratcheted MD simulations it is also possible to obtain information about the structure of the protein in the TS. In fact, the biasing force provided by the ratchet is positive along the reaction coordinate when the system is climbing a free-energy barrier, while it is zero when the system is descending it. Consequently, the TSs can be located by selecting the points of the trajectory where the biasing energy drops and the derivative of the extension of the molecule with respect to time peaks (Figure S6 and Supporting Information). The selected set of TS conformations was first analyzed in terms of end-to-end distance (Figure 4A). At 12 pN, the average distance between the native state and TS (d) is 5.8 ± 0.2 nm, in good agreement with the 5.4 ± 0.6 nm obtained experimentally (Table 1). The ensemble of conformations that represent the TS at 12 pN (Figure 4A) is structurally homogeneous, displaying an average root-mean-square deviation (RMSD) of 0.44 ± 0.22 nm. When only the structured regions of the TS are included the RMSD is 0.24 ± 0.03 nm. When simulations carried out at different forces are compared, the position of the TS along the unfolding coordinate appears to be force independent (Figure S7), validating the assumption made in the treatment of the experimental data (Supporting Information). The intrahelical contacts of H4, the structure of H2−H3 and some tertiary contacts between H2−H3 and H4 are still formed in the TS, while H1 is completely unfolded (Figure 4B).

Simulations of the mechanical denaturation of ACBP$^{46-86}$ were also attempted but they were not successful because a good reaction coordinate could not be found (see Supporting Information).

DISCUSSION

The significant pliability of the native state observed in our experiments is a hitherto undiscovered property of single-domain globular proteins. To date, the distance from N to TS in the unfolding reaction of ACBP is the largest reported for any single-domain globular protein structure. In the case of ACBP, having a deformable structure may be advantageous for its functions in the cell. ACBP binds acyl-CoA esters with a broad range of acyl-chain lengths (C_8−C_{24}), and the acyl-chain forms part of the binding site for the CoA headgroup.[56] The 3′-phosphate group alone accounts for 40% of the binding energy with specific interactions to conserved residues of ACBP[56,57]

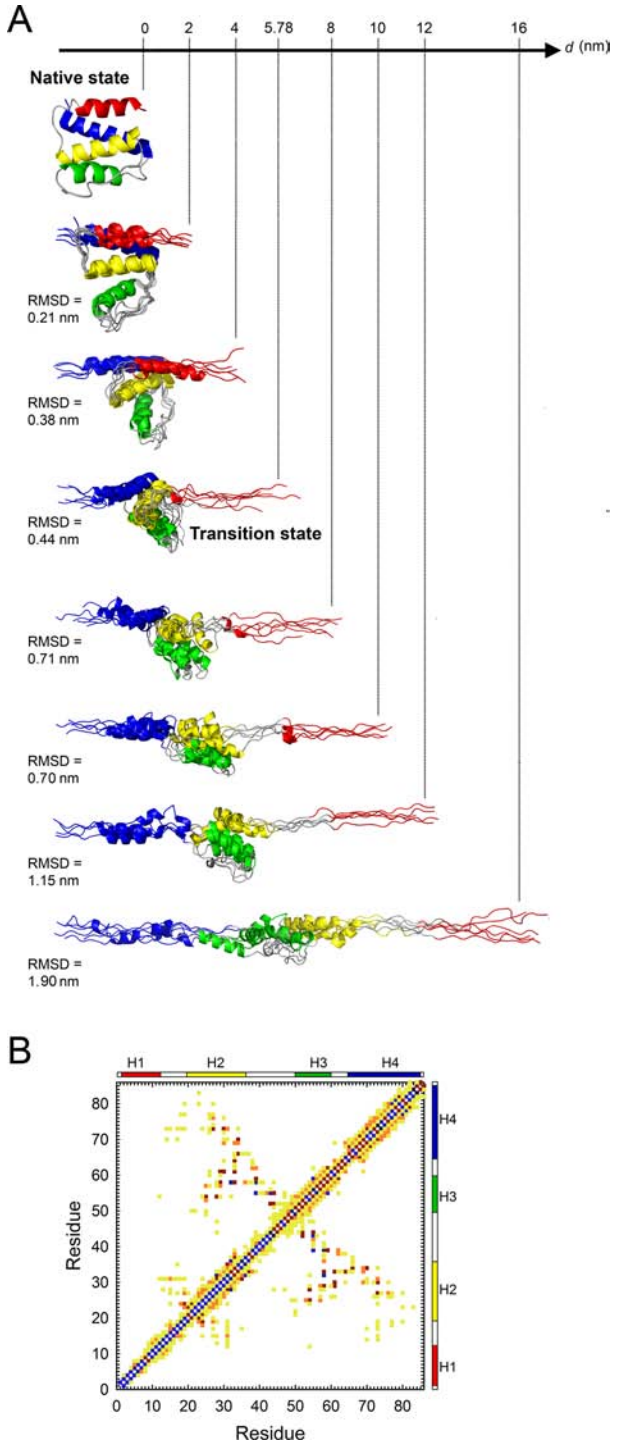

Figure 4. Molecular dynamics simulation of ACBP$^{1-86}$ forced unfolding. (A) Snapshots of the unfolding trajectories at force k = 12 pN, selected at different values of d, which represents the distance between the N- and C-termini of each molecular conformation relative to the native state. The structural variability (in terms of RMSD) associated with each value of d is indicated next to the snapshots. The TS structure is indicated at d = 5.78 nm. (B) The TS contact map. The colors indicate the average number of atomic contacts, light colors indicating low average and dark colors indicating high average.

dx.doi.org/10.1021/ja305862m | J. Am. Chem. Soc. 2012, 134, 17068−17075

and this necessitates its correct positioning. Acyl-chain exposure must furthermore be minimized, and hence is accommodated within the ACBP scaffold most likely through an adaptive induced fit. Functionally, ACBP is involved in fatty acid elongation as well as membrane assembly and formation,[58] positioning it in an environment likely to inflict strain on a structure. Hence, ACBP has built-in pliability important for both ligand binding and delivery in accordance to the one observed here. Such large native state compliance (large $x^{\ddagger}_{u}$) makes the unfolding rate very sensitive to force, as $k \propto \exp(Fx^{\ddagger}_{u}/k_{B}T)$. Proteins that are subjected to translocation or otherwise need to be unfolded take up less cellular energy if they are more sensitive to force. Compliance could even provide a mean to regulate these processes and thus be a source of evolutionary pressure.

What are the molecular determinants of protein structure pliability? In general, all-helical proteins have been found to have lower mechanical stability and larger compliance than β-sheet proteins, and fibrillar coiled coil structures have been shown to be exceptionally malleable.[11,48,59] This has been explained by the extensive hydrogen bonding in β-sheet proteins, which provides higher mechanical resistance than the longer range hydrophobic interactions that stabilize α-helical proteins.[60] However, the high compliance of ACBP cannot be attributed simply to its all-helical composition since several such proteins have been studied, both by experiment and computation, and found to have relatively brittle native states.[7,8,11,12,16,60] In fact, the compliance of previously studied proteins has been shown to correlate well with both contact order (CO) and helix content; yet ACBP is clearly anomalous as it fails to show correlation with these parameters (using CO or helix content for ACBP, $x^{\ddagger}_{u}$ should be ∼0.7 nm or ∼1.1 nm, respectively).[11] As an example, spectrin is a three-helix bundle of similar size as ACBP and its mechanical properties have been studied both experimentally (AFM) and computationally.[11,60] This protein, which serves to maintain the structural integrity of cells, was found to have a relatively large distance to the transition state (1.5 nm), with good agreement between experiment and simulation. Despite it being one of the most compliant structures determined with AFM it can be considered brittle when compared to ACBP. Nevertheless, despite the unusual mechanical properties of ACBP, its $x^{\ddagger}_{u}$ correlates well with its average unfolding force, as $F_{u}x^{\ddagger}_{u} \sim 530$ pNÅ. In fact, the product $F_{u}x^{\ddagger}_{u}$ has been shown to be a constant for proteins and emphasizes that mechanically stable proteins have short $x^{\ddagger}_{u}$ as they are less sensitive to force.[61,62]

In the case of molten globules, their large mechanical compliance has been ascribed to molecular structures mainly stabilized by short-range interactions and weak nonstereospecific tertiary contacts. This could suggest that the compliance of ACBP is due to fewer tertiary interactions or a lower relative CO (CO normalized with chain length) compared to other proteins.[63] However, a simple comparison of the CO of ACBP (CO ∼ 14%) with that of the similar α-helical proteins spectrin (CO ∼ 8% and $x^{\ddagger}_{u}$ = 1.5 nm)[64] and apomyoglobin (CO ∼ 8% and $x^{\ddagger}_{u}$ = 1.2 nm)[16] shows that this is not the case.

The origin of the large distance between N and TS of ACBP is not clear. However, one may speculate whether the unusual pliability of ACBP derives from either its unique fold and/or the strong helical propensity of H4. The four-helix bundle is a common fold in proteins but the up-down-down-up skewed bundle arrangement seen in ACBP is unique.[65] Also, predictions show that H4 has three times higher helical propensity than the other three helices and even the isolated helix peptide under denaturing conditions shows 24% helicity in solution.[34,66] Consequently, when force is applied on helices H1 and H4 (ACBP$^{1-86}$ variant), H1 can unfold completely before the structure of the H2−H3−H4 complex is mechanically altered, and thus before ACBP crosses the TS barrier. This process may be the origin of the large distance between N and TS. The strong helical propensity of H4 might also be the basis of the large compliance displayed by ACBP$^{46-86}$. However, the interpretation of these data is more difficult as no MD simulations are available.

Several studies have compared protein unfolding pathways observed during chemical/thermal and mechanical denaturation.[67,68] These studies have been performed using AFM or MD simulations with high unfolding forces or speeds, and the general emerging conclusion is that the forced and zero-force unfolding pathways are not the same.[20−22] However, AFM experiments using filamin have suggested parallel unfolding pathways to exist at low pulling speeds[69] and MD simulations have shown that at low forces a pathway-switch occurs where the forced unfolding pathways start to resemble those observed during thermal denaturation.[23] This force-based switch-effect has also been explored numerically for the protein fibronectin in the intermediate force/speed regime with an all-atom model[70] and in the low-force regime with a simplified model.[71] The results of these studies have shown that in the low to intermediate force/speed regime, the protein landscape is still rough, exhibiting several local minima and maxima which act as kinetic traps with the protein fluctuating between them, while at large force/speed the landscape is completely flattened by the external perturbation, leading to a predominant unfolding pathway.

Here, we used ratcheted MD simulations to follow the forced unfolding pathway of ACBP at low forces. Interestingly, the TS observed in our simulations resembles that observed in bulk using chemical denaturation. Several residues that form contacts in the mechanical TS are the same that form native contacts in the zero-force TS, as identified by phi-value analysis.[72,73] In fact, more recent studies have suggested that the complex H2−H3−H4 is formed in the TS populated in bulk as it is in the mechanical TS.[74] Some differences might concern H1 as this helix is completely unfolded in the mechanical TS, while in bulk studies, it might be at least partially folded in the chemically induced TS as interactions between H1 and H2−H4 have been observed.[72] However, both in the mechanical and chemical unfolding H1 appears to be the least stable and the first helix to lose structure.[75] Thus, although the mechanical TS might be less native-like than the chemical TS, the sequence of events leading to the unfolding of ACBP appears to be similar. This conclusion is supported by the position of TS along the reaction coordinate. The mβ_{T}-value is analogous to the Tanford value (β_{T}) used in chemical denaturation studies.[16,17] For the spontaneous refolding of ACBP, β_{T} was determined to be 0.61 ± 0.02.[63,76] This value compares well with the mβ_{Tf} of 0.55 ± 0.06 deduced from our experiments.

The gentle mechanical manipulation that is possible to achieve with a low spring-constant optical trap might favor sampling of the same unfolding pathways as are populated in bulk studies. However, the observed similarities between forced and spontaneous unfolding of ACBP might be specific to this molecule. In fact, other proteins have been manipulated in the low-force regime with optical tweezers and displayed much

shorter $x^{\ddagger}_{u}$ (<2 nm).[7,12,16] The structure of ACBP is simple and at the same time unique. Among its four helices, H1 appears to be the weakest both under mechanical and chemical perturbation, while H4 is the strongest. The sequence of events leading to the denaturation of ACBP might be mostly determined by the remarkable difference in stability between these two helices regardless of the denaturant. Thus, the behavior of ACBP under tension could originate from the unique properties of this molecule and might be observed only with proteins that have similar structural features.

CONCLUSIONS

Our studies show that native state protein structures can be much more pliant to force than previously anticipated. To our knowledge, ACBP is the most compliant globular single-domain protein structure characterized so far in force spectroscopy experiments. Our studies also provide the first experimental evidence of a spontaneous-like mechanical unfolding pathway of a protein. The TS populated by $ACBP^{1-86}$ during mechanical unfolding compares well with that populated in bulk studies, both for its position along the reaction coordinate and for its structure. The results presented here disclose a new type of response to force of a protein native state which may be important for protein function and biomaterial design.

Abbreviations. ACBP, acyl-CoA binding protein; AFM, atomic force microscopy; CO, contact order; CoA, coenzyme A; MD, molecular dynamics; RMSD, root mean square deviation; N, native state; TS, transition state; U, unfolded state.

ASSOCIATED CONTENT

Supporting Information

Figures showing fitting to the WLC model, fitting of unfolding/refolding distributions to a probability distribution function, the force-jump experiment, force and dwell-time distributions for $ACBP^{46-86}$ and fitting to a probability distribution function, contact map for the sequence of unfolding events in the MD simulations, location of the TS in MD simulations, TS position as a function of force in MD simulation, text describing details of MD simulations. This material is available free of charge via the Internet at http://pubs.acs.org.

AUTHOR INFORMATION

Corresponding Author

ciro.cecconi@gmail.com

Notes

The authors declare no competing financial interest.

ACKNOWLEDGMENTS

P.O.H., F.M.P., and B.B.K. acknowledge the Carlsberg Foundation for financial support (no. 2008-01-0368). C. Camilloni was supported by a Long Term FEBS Fellowship and a Marie Curie Intra-European Fellowship. A.I. gratefully acknowledges financial support from the Lundbeck Foundation. C. Cecconi gratefully acknowledges financial support from Fondazione Cassa di Risparmio di Modena, the EU through a Marie Curie International Re-Integration Grant (no. 44952) and the Italian MIUR (Grant no. 17DPXLNBEK). P. Skovgaard is thanked for technical assistance. We also thank Prof. E. Molinari and Drs. P. Facci and K. Teilum for their insightful discussions. We thank Dr. S. Smith, Dr. C. Ascoli, and Dr. M. Nakaema for their contributions to the development of the optical tweezers setup. We honor the memory of Flemming M. Poulsen who passed away during the preparation of this article.

REFERENCES

(1) Bustamante, C.; Chemla, Y. R.; Forde, N. R.; Izhaky, D. *Annu. Rev. Biochem.* **2004**, *73*, 705.
(2) Lu, H.; Schulten, K. *Proteins* **1999**, *35*, 453.
(3) Doherty, G. J.; McMahon, H. T. *Annu. Rev. Biophys.* **2008**, *37*, 65.
(4) Maillard, R. A.; Chistol, G.; Sen, M.; Righini, M.; Tan, J.; Kaiser, C. M.; Hodges, C.; Martin, A.; Bustamante, C. *Cell* **2011**, *145*, 459.
(5) Jaalouk, D. E.; Lammerding, J. *Nat. Rev. Mol. Cell Biol.* **2009**, *10*, 63.
(6) Borgia, A.; Williams, P. M.; Clarke, J. *Annu. Rev. Biochem.* **2008**, *77*, 101.
(7) Cecconi, C.; Shank, E. A.; Bustamante, C.; Marqusee, S. *Science* **2005**, *309*, 2057.
(8) Stigler, J.; Ziegler, F.; Gieseke, A.; Gebhardt, J. C.; Rief, M. *Science* **2011**, *334*, 512.
(9) Bechtluft, P.; van Leeuwen, R. G.; Tyreman, M.; Tomkiewicz, D.; Nouwen, N.; Tepper, H. L.; Driessen, A. J.; Tans, S. J. *Science* **2007**, *318*, 1458.
(10) Ng, S. P.; Clarke, J. *J. Mol. Biol.* **2007**, *371*, 851.
(11) Li, M. S. *Biophys. J.* **2007**, *93*, 2644.
(12) Shank, E. A.; Cecconi, C.; Dill, J. W.; Marqusee, S.; Bustamante, C. *Nature* **2010**, *465*, 637.
(13) Xi, Z.; Gao, Y.; Sirinakis, G.; Guo, H.; Zhang, Y. *Proc. Natl. Acad. Sci. U.S.A.* **2012**, *109*, 5711.
(14) Oberhauser, A. F.; Badilla-Fernandez, C.; Carrion-Vazquez, M.; Fernandez, J. M. *J. Mol. Biol.* **2002**, *319*, 433.
(15) Sadler, D. P.; Petrik, E.; Taniguchi, Y.; Pullen, J. R.; Kawakami, M.; Radford, S. E.; Brockwell, D. J. *J. Mol. Biol.* **2009**, *393*, 237.
(16) Elms, P. J.; Chodera, J. D.; Bustamante, C.; Marqusee, S. *Proc. Natl. Acad. Sci. U.S.A.* **2012**, *109*, 3796.
(17) Tanford, C. *Adv. Protein Chem.* **1970**, *24*, 1.
(18) Brockwell, D. J.; Beddard, G. S.; Paci, E.; West, D. K.; Olmsted, P. D.; Smith, D. A.; Radford, S. E. *Biophys. J.* **2005**, *89*, 506.
(19) Lee, W.; Zeng, X.; Rotolo, K.; Yang, M.; Schofield, C. J.; Bennett, V.; Yang, W.; Marszalek, P. E. *Biophys. J.* **2012**, *102*, 1118.
(20) Fowler, S. B.; Best, R. B.; Toca Herrera, J. L.; Rutherford, T. J.; Steward, A.; Paci, E.; Karplus, M.; Clarke, J. *J. Mol. Biol.* **2002**, *322*, 841.
(21) Best, R. B.; Fowler, S. B.; Herrera, J. L.; Steward, A.; Paci, E.; Clarke, J. *J. Mol. Biol.* **2003**, *330*, 867.
(22) Ng, S. P.; Rounsevell, R. W.; Steward, A.; Geierhaas, C. D.; Williams, P. M.; Paci, E.; Clarke, J. *J. Mol. Biol.* **2005**, *350*, 776.
(23) West, D. K.; Olmsted, P. D.; Paci, E. *J. Chem. Phys.* **2006**, *124*, 154909.
(24) Imparato, A.; Pelizzola, A. *Phys. Rev. Lett.* **2008**, *100*, 158104.
(25) Kleiner, A.; Shakhnovich, E. *Biophys. J.* **2007**, *92*, 2054.
(26) Imparato, A.; Pelizzola, A.; Zamparo, M. *Phys. Rev. Lett.* **2007**, *98*, 148102.
(27) Serquera, D.; Lee, W.; Settanni, G.; Marszalek, P. E.; Paci, E.; Itzhaki, L. S. *Biophys. J.* **2010**, *98*, 1294.
(28) Arad-Haase, G.; Chuartzman, S. G.; Dagan, S.; Nevo, R.; Kouza, M.; Mai, B. K.; Nguyen, H. T.; Li, M. S.; Reich, Z. *Biophys. J.* **2010**, *99*, 238.
(29) Marchi, M.; Ballone, P. *J. Chem. Phys.* **1999**, *110*, 3697.
(30) Paci, E.; Karplus, M. *J. Mol. Biol.* **1999**, *288*, 441.
(31) Paci, E.; Karplus, M. *Proc. Natl. Acad. Sci. U.S.A.* **2000**, *97*, 6521.
(32) Camilloni, C.; Broglia, R. A.; Tiana, G. *J. Chem. Phys.* **2011**, *134*, 045105.
(33) Andersen, K. V.; Poulsen, F. M. *J. Biomol. NMR* **1993**, *3*, 271.
(34) Teilum, K.; Kragelund, B. B.; Poulsen, F. M. *J. Mol. Biol.* **2002**, *324*, 349.
(35) Mandrup, S.; Hojrup, P.; Kristiansen, K.; Knudsen, J. *Biochem. J.* **1991**, *276* (Pt3), 817.

(36) Cecconi, C.; Shank, E. A.; Dahlquist, F. W.; Marqusee, S.; Bustamante, C. *Eur. Biophys. J.* **2008**, *37*, 729.
(37) Smith, S. B.; Cui, Y.; Bustamante, C. *Methods in enzymology* **2003**, *361*, 134.
(38) Marszalek, P. E.; Li, H.; Oberhauser, A. F.; Fernandez, J. M. *Proc. Natl. Acad. Sci. U.S.A.* **2002**, *99*, 4278.
(39) Schlierf, M.; Li, H.; Fernandez, J. M. *Proc. Natl. Acad. Sci. U.S.A.* **2004**, *101*, 7299.
(40) Li, P. T.; Collin, D.; Smith, S. B.; Bustamante, C.; Tinoco, I., Jr. *Biophys. J.* **2006**, *90*, 250.
(41) Liphardt, J.; Onoa, B.; Smith, S. B.; Tinoco, I., Jr.; Bustamante, C. *Science* **2001**, *292*, 733.
(42) Bell, G. I. *Science* **1978**, *200*, 618.
(43) Wen, J. D.; Manosas, M.; Li, P. T.; Smith, S. B.; Bustamante, C.; Ritort, F.; Tinoco, I., Jr. *Biophys. J.* **2007**, *92*, 2996.
(44) Manosas, M.; Wen, J. D.; Li, P. T.; Smith, S. B.; Bustamante, C.; Tinoco, I., Jr.; Ritort, F. *Biophys. J.* **2007**, *92*, 3010.
(45) Dudko, O. K.; Hummer, G.; Szabo, A. *Phys. Rev. Lett.* **2006**, *96*, 108101.
(46) Dudko, O. K.; Hummer, G.; Szabo, A. *Proc. Natl. Acad. Sci. U.S.A.* **2008**, *105*, 15755.
(47) Garcia-Manyes, S.; Dougan, L.; Badilla, C. L.; Brujic, J.; Fernandez, J. M. *Proc. Natl. Acad. Sci. U.S.A.* **2009**, *106*, 10534.
(48) Gebhardt, J. C.; Bornschlogl, T.; Rief, M. *Proc. Natl. Acad. Sci. U.S.A.* **2010**, *107*, 2013.
(49) Evans, E.; Ritchie, K. *Biophys. J.* **1997**, *72*, 1541.
(50) Duan, Y.; Wu, C.; Chowdhury, S.; Lee, M. C.; Xiong, G.; Zhang, W.; Yang, R.; Cieplak, P.; Luo, R.; Lee, T.; Caldwell, J.; Wang, J.; Kollman, P. *J. Comput. Chem.* **2003**, *24*, 1999.
(51) DePaul, A. J.; Thompson, E. J.; Patel, S. S.; Haldeman, K.; Sorin, E. J. *Nucleic Acids Res.* **2010**, *38*, 4856.
(52) Van Der Spoel, D.; Lindahl, E.; Hess, B.; Groenhof, G.; Mark, A. E.; Berendsen, H. J. *J. Comput. Chem.* **2005**, *26*, 1701.
(53) Camilloni, C.; Provasi, D.; Tiana, G.; Broglia, R. A. *Proteins* **2008**, *71*, 1647.
(54) Teilum, K.; Poulsen, F. M.; Akke, M. *Proc. Natl. Acad. Sci. U.S.A.* **2006**, *103*, 6877.
(55) Teilum, K.; Maki, K.; Kragelund, B. B.; Poulsen, F. M.; Roder, H. *Proc. Natl. Acad. Sci. U.S.A.* **2002**, *99*, 9807.
(56) Kragelund, B. B.; Andersen, K. V.; Madsen, J. C.; Knudsen, J.; Poulsen, F. M. *J. Mol. Biol.* **1993**, *230*, 1260.
(57) Faergeman, N. J.; Sigurskjold, B. W.; Kragelund, B. B.; Andersen, K. V.; Knudsen, J. *Biochemistry* **1996**, *35*, 14118.
(58) Gaigg, B.; Neergaard, T. B.; Schneiter, R.; Hansen, J. K.; Faergeman, N. J.; Jensen, N. A.; Andersen, J. R.; Friis, J.; Sandhoff, R.; Schroder, H. D.; Knudsen, J. *Mol. Biol. Cell* **2001**, *12*, 1147.
(59) Gao, Y.; Sirinakis, G.; Zhang, Y. *J. Am. Chem. Soc.* **2011**, *133*, 12749.
(60) Schlierf, M.; Rief, M. *J. Mol. Biol.* **2005**, *354*, 497.
(61) Dietz, H.; Rief, M. *Phys. Rev. Lett.* **2008**, *100*, 098101.
(62) Kumar, S.; Li, M. S. *Phys. Rep.* **2010**, *486*, 1.
(63) Plaxco, K. W.; Simons, K. T.; Baker, D. *J. Mol. Biol.* **1998**, *277*, 985.
(64) Rief, M.; Pascual, J.; Saraste, M.; Gaub, H. E. *J. Mol. Biol.* **1999**, *286*, 553.
(65) Kragelund, B. B.; Knudsen, J.; Poulsen, F. M. *Biochim. Biophys. Acta* **1999**, *1441*, 150.
(66) Fieber, W.; Kragelund, B. B.; Meldal, M.; Poulsen, F. M. *Biochemistry* **2005**, *44*, 1375.
(67) Carrion-Vazquez, M.; Oberhauser, A. F.; Fowler, S. B.; Marszalek, P. E.; Broedel, S. E.; Clarke, J.; Fernandez, J. M. *Proc. Natl. Acad. Sci. U.S.A.* **1999**, *96*, 3694.
(68) Cao, Y.; Li, H. *J. Mol. Biol.* **2008**, *375*, 316.
(69) Yew, Z. T.; Schlierf, M.; Rief, M.; Paci, E. *Phys. Rev. E: Stat., Nonlinear, Soft Matter Phys.* **2010**, *81*, 031923.
(70) Mitternacht, S.; Luccioli, S.; Torcini, A.; Imparato, A.; Irback, A. *Biophys. J.* **2009**, *96*, 429.
(71) Caraglio, M.; Imparato, A.; Pelizzola, A. *J. Chem. Phys.* **2010**, *133*, 065101.
(72) Kragelund, B. B.; Osmark, P.; Neergaard, T. B.; Schiodt, J.; Kristiansen, K.; Knudsen, J.; Poulsen, F. M. *Nat. Struct. Biol.* **1999**, *6*, 594.
(73) Teilum, K.; Thormann, T.; Caterer, N. R.; Poulsen, H. I.; Jensen, P. H.; Knudsen, J.; Kragelund, B. B.; Poulsen, F. M. *Proteins* **2005**, *59*, 80.
(74) Bruun, S. W.; Iesmantavicius, V.; Danielsson, J.; Poulsen, F. M. *Proc. Natl. Acad. Sci. U.S.A.* **2010**, *107*, 13306.
(75) Kragelund, B. B.; Heinemann, B.; Knudsen, J.; Poulsen, F. M. *Protein Sci.* **1998**, *7*, 2237.
(76) Kragelund, B. B.; Hojrup, P.; Jensen, M. S.; Schjerling, C. K.; Juul, E.; Knudsen, J.; Poulsen, F. M. *J. Mol. Biol.* **1996**, *256*, 187.